Anderson localisation of visible light on a nanophotonic chip

Tom Crane,[†,‡] Oliver Joe Trojak,[†,‡] Juan Pablo Vasco,[¶] Stephen Hughes,[¶] and Luca Sapienza[*,†]

E-mail: l.sapienza@soton.ac.uk

Abstract

Technological advances allow the control of light at the nanoscale and to strongly enhance the light-matter interaction in highly engineered devices. Enhancing the light-matter interaction is needed for applications in research areas such as quantum technology, energy harvesting, sensing and biophotonics. Here, we show that a different approach, based on the use of disorder rather than the precise engineering of the devices and that utilises fabrication imperfections as a resource, can allow the efficient trapping of visible light on a chip. We demonstrate, for the first time to our knowledge, Anderson-localisation of light at visible wavelengths in a nanophotonic chip. Remarkably, we prove that disorder-induced localisation is more efficient in confining visible light than highly engineered optical cavities, thus reversing the trend observed so far. We measure light-confinement quality factors approaching 10000 that are significantly higher than values previously reported in two-dimensional photonic crystals. These

[*]To whom correspondence should be addressed

[†]Department of Physics and Astronomy, University of Southampton, Southampton SO17 1BJ, United Kingdom

[‡]Equal contribution

[¶]Department of Physics, Queen's University, Kingston, Ontario, K7L 3N6 Canada

measurements are well explained using a three-dimensional Bloch mode expansion technique, where we also extract the mode quality factors and effective mode volume distributions of the localised modes. Furthermore, by implementing a sensitive imaging technique, we directly visualise the localised modes and measure their spatial extension. Even though the position where the cavities appear is not controlled, given the multiple scattering process at the basis of their formation, we are able to locate with nanometer scale accuracy the position of the optical cavities. This is important for the deterministic coupling of emitters to the disorder-induced optical cavities and for assessing light localisation. Our results show the potential of disorder as a novel resource for the efficient confinement of light and for the enhancement of the light-matter interaction in the visible range of wavelengths.

Keywords

Anderson localisation, visible light, nanophotonic devices, photonic crystals, multiple scattering, nanofabrication, disordered photonics, on-chip optical cavities

Being able to control light propagation is of tremendous interest for a variety of applications,[1] including energy harvesting,[2] sensing,[3] drug delivery[4] and quantum information technology.[5] Technological advances allow to control light at the nanoscale and to strongly enhance the light-matter interaction in highly engineered devices. However, the requirement of highly accurate fabrication techniques[6] often limits the scalability and wide application of such devices. Surprisingly, an alternative to highly engineered cavities for the confinement of waves exists. Whenever imperfections or defects are present, a wave propagating through a medium can undergo multiple scatterings. If the amount of scattering is strong enough, the wave can be trapped and its propagation can even come to a complete stop. A phase transition from ballistic propagation to localisation can thus occur[7] and we can enter the realm of Anderson localisation.[8] Such a regime can be sustained by any kind of wave and

has been demonstrated for electrons, sound waves, Bose-Einstein condensates and infrared optical waves.[9]

So far, photonic devices based on Anderson localisation have been mostly developed in the near-infrared range of wavelengths, in particular in the telecommunication band in silicon,[10–12] where optical losses are the lowest, and in gallium arsenide samples containing light emitters.[13–15] In this work, we demonstrate, for the first time to our knowledge, Anderson localisation of visible light on a nanophotonic chip. The use of multiple scattering of visible light has exciting prospects in a range of applications, following, for instance, theoretical predictions in energy harvesting[16] and proof-of-principle results in imaging.[17]

A technological challenge in nanophotonic devices operating at visible wavelength, compared to longer wavelength near-infrared devices, lies in the smaller feature sizes that need to be fabricated. Also, losses at visible wavelengths are higher than, for instance, at telecommunication wavelengths in silicon-based materials, which implies that high-quality confinement of visible light can be more difficult to achieve. Despite such challenges, we demonstrate Anderson localisation of visible light on a nanophotonic chip. We prove that making use of fabrication imperfections in devices operating at visible wavelengths is a novel route for achieving quality factors that can be up to one order of magnitude larger than in highly-engineered devices. This is an unprecedented result since, so far, quality factors measured in Anderson-localised cavities operating in the near-infrared range of wavelengths have been orders of magnitude lower than engineered planar photonic crystal ones, as discussed in more detail below. Our work shows that Anderson localisation can be utilized to substantially increase the light-matter interaction at visible wavelengths; this is particularly relevant for energy harvesting, sensing, biology and quantum information technology applications with emitters operating in the visible.

We investigate light localisation by structural disorder on a nanophotonic chip, comprising photonic crystal waveguides in which disorder is due to intrinsic fabrication imperfections and/or to a random displacement that we introduce in the position of the air holes with re-

spect to the perfectly periodic photonic crystal structure. The effect of disorder in photonic crystal waveguides is now known to play a profoundly important role on the slow light Bloch modes, resulting in enhanced backscatter losses[18,19] and multiple scattering.[20] This work shows how multiple scattering of light on imperfections can be used as a resource to confine visible light efficiently on a chip, with performances that even surpass those of highly engineered devices. Our results prove that, by means of nanofabrication, optical imaging and photo-luminescence measurements, we are able to achieve Anderson localisation, locate Anderson-localised modes with sub-micron accuracy, study their spatial extension and demonstrate efficient confinement of visible light in a chip that exceeds the state-of-the-art. Such devices are more scalable than standard photonic crystal cavities, since nanoscale accuracy in the fabrication process is not required and tens of high-quality optical cavities appear along a single photonic crystal waveguide. Our results open an alternative path to applications requiring enhanced light-matter interaction in the visible, for instance in biophysics, single-molecule spectroscopy, optical sensing and quantum technology.

Silicon nitride is an advantageous material for photonic applications given its compatibility with existing semiconductor fabrication technology and its transparency to a wide range of wavelengths, including the visible. Examples of its applications include integrated non-linear optics[21] and opto-mechanical[22] devices. Depending on the growth technique used, silicon nitride can host defect centres with various levels of brightness that can exhibit a broad luminescence, covering wavelengths that typically range from about 500 to 800 nm.[23] Taking advantage of this, we have fabricated suspended silicon nitride photonic crystal waveguides on a silicon substrate (for more details on the fabrication process, see Methods section) and used the material's light emission to reveal the formation of localised modes due to the multiple scattering of light on imperfections. Using the intrinsic photo-luminescence, we image and spectrally characterise disorder-induced localised modes: to our knowledge, this is the first demonstration of Anderson localisation of visible light and of its direct imaging on a chip. Remarkably, the quality factor of the disorder-induced light confinement exceeds record

values so far reported for highly engineered two-dimensional photonic crystal heterostructure cavities,[24] making it a resource for enhanced light-matter interaction on a chip.

We use a room-temperature confocal micro-photoluminescence set-up (see Fig. 1a) where two light sources, a blue (455 nm central wavelength) light emitting diode (LED) and a 473 nm continuous-wave laser, are focused to illumination areas with diameters of approximately 50 μm and 2 μm respectively, on a sample placed on an xy-positioner. The LED is used to excite the photo-luminescence that is then imaged with an Electron Multiplying Charge Coupled Device (EMCCD).[26] The laser is used to locally excite the waveguides, whose emission is then spectrally characterised via a grating spectrometer equipped with a silicon CCD. An example of the broad-range photo-luminescence spectrum measured from the bulk silicon nitride sample under investigation is shown in Fig. 1b.

By means of finite-difference time-domain simulations and guided mode expansion technique, we design perfectly periodic suspended photonic crystal waveguides that confine light in the visible (the photonic band digram is shown in Fig. 1c). When disorder (beyond intrinsic disorder) is introduced in a photonic crystal waveguide, for instance by displacing the position and/or modifying the shape of the air holes, light propagation can be strongly affected and localisation can occur, giving rise to sharp spectral resonances.[19,27,28] To this end, we fabricate photonic crystal waveguides with different amounts of disorder, introduced by randomly displacing the air holes in the 3 (out of 20) rows of holes closest to the row of missing holes in the photonic crystal structure. The displacement distances are obtained from a Gaussian distribution with a varying standard deviation, expressed as percentage of the photonic crystal lattice parameter a (see Fig. 1d).

The waveguides are illuminated with the blue LED and the photo-luminescence images are collected by the EMCCD, as shown in Fig. 2a. When imaging waveguides where no intentional disorder is introduced, we observe a bright photo-luminescence signal from the central waveguide channel, proving the successful guiding of light along the line defect in the photonic crystal structure. When disorder is deliberately introduced in the system, localised

areas of higher intensity are visible along the waveguide, which are the indication of light confinement within optical cavities in the Anderson-localised regime (see Fig. 2a, left panels). Thanks to the spontaneous luminescence of the silicon nitride material that acts as a homogenous internal light source, we can observe the confined optical modes directly in the photo-luminescence images, without the need to reconstruct an image via the scanning of a laser spot [13] or the use of sophisticated techniques like near-field scanning optical microscopy or cathodo-luminescence. We can thus visualise the Anderson-localised modes, locate their position with nanometer accuracy and evaluate their far-field spatial extension. From the linecuts of the photo-luminescence images, we can extract the far-field spatial extension of the modes, as shown in the right panels of Fig. 2a. By analysing the statistics as a function of disorder (see Fig. 2b), we observe that the extensions of the optical resonances, each characterised by a specific spectral signature, all lie below 1.2 μm. These values are significantly shorter than the 100 μm-length of the fabricated waveguides, thus proving localisation.

Even though, due to the multiple scattering process at the basis of the formation of the disorder-induce localised cavities, we cannot predict where the confined modes will appear along the waveguides, our technique allows to precisely locate Anderson-localised "cavities" and measure their confined optical wavelength and spatial extension. This allows a thorough characterization of the properties of disorder-induced light confinement and opens up the possibility of deterministically coupling emitters via local deposition onto specific optical modes.

By locally exciting the sample with the laser source, we can probe specific positions along the waveguides and spectrally characterise the emission of selected localised modes. Sharp resonances, the signature of light confinement in optical cavities, clearly appear superimposed on the broad silicon nitride photo-luminescence. These resonances appear in proximity to the guided modes band edges, calculated for the perfectly periodic photonic crystal structure employing the guided mode expansion technique, as expected for disorder-induced localised light (see Fig. 1c). [10,13] Light is localised if the variance of the normalized

intensity distribution exceeds the critical value of 7/3:[13,29] we extract a variance of 3.3, thus proving Anderson localisation (see Fig. 3a). When scanning the laser along the waveguide, multiple resonances appear at different wavelengths, as expected from confinement due to a multiple-scattering process. Several resonances can be observed in each spectrum, when more than one mode lies within the excitation spot of our laser that has a diameter of approximately 2 μm. As such, large numbers of cavities can appear along each 100 μm-long photonic crystal waveguide. We measure linewidths $\Delta\lambda$ of the resonances as low as 0.08 nm, reaching quality factors $Q = \lambda/\Delta\lambda$ (where λ is the central wavelength of the spectral peak) of the confined light as high as 9300 ± 800 (see Fig. 3c-f). This value largely surpasses ones reported for engineered two-dimensional photonic crystal cavities in silicon nitride, where typical experimental quality factors range between a few hundred[30] and one thousand,[31,32] and even exceeds the previous record value of a few thousand reported for an highly-engineered photonic crystal heterostructure cavity.[24] To our knowledge, this represents the highest quality factor reported for two-dimensional photonic crystal cavities in the visible range of wavelengths (though higher values been reported in non planar structures like photonic crystal nanobeams[25]). If we consider the ratio Q_A/Q_{2D} between the highest quality factors reported for Anderson-localised and engineered two-dimensional cavities, at telecom wavelengths this ratio has the value of $\sim$0.02,[10,33] in the near-infrared $\sim$0.3,[13,34] while in the visible we reach $\sim$3,[24] thus reversing the trend reported so far. Remarkably, we show that disorder-induced localisation of light provides quality factors exceeding those of engineered cavities, proving the potential of disorder for enhanced on-chip light-matter interaction.

In our devices, the existence of optical cavities relies on light being trapped by scattering on imperfections: a distribution of cavity wavelengths and quality factors is therefore expected and an example of its statistics is shown in Fig. 3g. Fabricating devices with different degrees of disorder allows us to study the dependence of the quality factor of the light confinement on disorder: we measure quality factors between $\sim$100 and $\sim$10000 that decrease when the level of imperfection in the system is increased. This is compatible with previous

reports[13] and can be attributed to the fact that, if more defects are present, the probability for light to be scattered out of the cavity increases, thus reducing the light-confinement quality factor. As shown in Fig. 3g, the intrinsic fabrication imperfections (0 % deliberate disorder) are enough to provide high-quality light confinement and no engineering of the disorder is required in order to achieve the optimal operation condition for the fabricated devices.

To corroborate our experiments, we have applied a fully three-dimensional Bloch mode expansion technique to compute the quality factors and mode volume distributions of the disordered waveguides.[27,28] The value of intrinsic disorder, obtained by fitting the experimental results measured from the samples where no intentional disorder was introduced, was found to be $0.02a$ (where a is the lattice constant). The histograms in Fig. 3g represent the mean quality factors calculated for the different degrees of disorder, showing a very good agreement with our experimental results. An example of the calculated mode profile for an Anderson-localised mode, is shown in the inset of Fig. 3b, together with the effective mode volume distributions calculated for 0, 4, 8 % disorder. From the calculations, the mode volumes of Anderson-localised cavities[27] appear to be below $4(\lambda/n)^3$, where λ is the wavelength of light and n is the refractive index of the material, values that are indeed very promising for enhanced light-matter coupling of single emitters in cavity quantum electrodynamics experiments.[35]

In conclusion, we have demonstrated Anderson localisation of visible light on a silicon nitride chip and, by means of photo-luminescence imaging, we have visualised the confined optical modes. Despite the lack of control of the position of the optical cavities due to the multiple scattering process fundamental to the formation of the disorder-induced localised modes, we have shown that once the devices are fabricated, our technique allows the location of the optical cavities with nanometer accuracy. This represents an important step towards the deterministic addressing of disordered photonic cavities. Photoluminescence imaging also allows extracting the localised modes far-field spatial extension, an important param-

eter for assessing light localisation. The spectral characterisation of the disorder-induced localised modes in our nanophotonic devices has revealed confinements with record quality factors reaching ∼10000, exceeding, for the first time, values reported for engineered two-dimensional photonic crystal cavities. High quality in the confinement of visible light can find applications in energy harvesting, imaging, sensing and fundamental research in light-matter interaction, for instance in random lasers[36] and cavity quantum electrodynamics experiments with emitters in the visible range, such as colloidal quantum dots,[37] defect centres in two-dimensional materials[38] and in diamond.[39] The latter are particularly attractive for quantum technology applications, thanks to their room temperature operation and spin-coherence properties.[40] Since diamond is a very difficult material to process, hybrid silicon-diamond structures are appealing to control light propagation and the spontaneous emission rate of defect centres.[41] Furthermore, given that many spatially-extended photonic modes spontaneously appear along the waveguides, their mutual overlap could be used to realise quantum information networks for the propagation of quantum light,[42] based on coupled Anderson-localised photonic modes, known as necklace states.[43] Room temperature operation also guarantees compatibility with biological systems with energy transitions occuring in the visible range of wavelengths, such as chromophores[44] and proteins,[45] whose light emission and absorption can be strongly enhanced by the coupling to high-quality optical cavities.

Methods

A 250 nm-thick silicon nitride layer is deposited on a silicon substrate via plasma-enhanced chemical vapor deposition, using a combination of SiH_4 and NH_3 gases at a temperature of 350°C and a pressure of 750 mTorr. Electron-beam lithography is used to write the photonic crystal pattern and an inductively coupled plasma reactive ion etch, based on SF_6 and C_4F_8, transfers the pattern onto the silicon nitride layer. A KOH wet etch is used to undercut

the silicon nitride, creating a free-standing photonic crystal membrane with nominal lattice constant $a = 310\,\mathrm{nm}$, hole radius $r = 110\,\mathrm{nm}$ and thickness $t = 250\,\mathrm{nm}$. We fabricate photonic crystal waveguides with different amounts of disorder, introduced by randomly displacing the air holes in the 3 (out of 20) rows of holes closest to the row of missing holes in the photonic crystal structure. The displacement distances are obtained from a Gaussian distribution with a varying standard deviation, expressed as percentage of the photonic crystal lattice parameter a.

Acknowledgments

We would like to thank Kartik Srinivasan for his continuous support and for the critical reading of the manuscript, Marcelo Davanço for useful discussions and Henry Nelson for his early contribution to this work.

References

(1) Vahala K. J. Optical microcavities. *Nature* **2003**, 424, 839-8463.

(2) Parida B.; Iniyan S.; Goic R. A review of solar photovoltaic technologies. *Renewable Sustainable Energy Rev.* **2011**, 15, 1625-1636.

(3) Hodgkinson J.; Tatam R. P. Optical gas sensing: a review. *Meas. Sci. Technol.* **2013**, 24, 012004.

(4) Sortino S. Photoactivated nanomaterials for biomedical release applications. *J. Mater. Chem.* **2012**, 22, 301-318.

(5) O'Brien J. L.; Furusawa A.; Vučković J. Photonic quantum technologies. *Nat. Photonics* **2009**, 3, 687-695.

(6) Akahane Y.; Asano T.; Song B.-S.; Noda S. High-Q photonic nanocavity in a two-dimensional photonic crystal, *Nature*, **2003**, 425, 944-947.

(7) Sheng P. *Introduction to wave scattering, localisation and mesoscopic phenomena*; Springer, 2006.

(8) Anderson P. W. Absence of diffusion in certain random lattices. *Phys. Rev.* **1958**, 109, 1492-1505.

(9) Lagendijk A.; van Tiggelen B.; Wiersma D. S. Fifty years of Anderson localization. *Phys. Today* **2009**, 62, 24-29.

(10) Topolancik J.; Ilic B.; Vollmer F. Experimental observation of strong photon localization in disordered photonic crystal waveguides. *Phys. Rev. Lett.* **2007**, 99, 253901.

(11) Mookherjea S.; Ong J. R.; Lou X.; Guo-Qiang L. Electronic control of optical Anderson localization modes. *Nat. Nanotechnol.* **2014**, 9, 365-371.

(12) Hsieh P.; Chung C.; McMillan J. F.; Tsai M.; Lu M.; Panoiu N. C.; Wong C. W. Photon transport enhanced by transverse Anderson localization in disordered superlattices. *Nat. Phys.* **2015**, 11, 268-274.

(13) Sapienza L.; Thyttestrup H.; Stobbe S.; Garcia P. D.; Smolka S.; Lodahl P. Cavity quantum electrodynamics with Anderson-localized modes. *Science* **2010**, 327, 1352-1355.

(14) Riboli F.; Caselli N.; Vignolini S.; Intonti F.; Vynck K.; Barthelemy P.; Gerardino A.; Balet L.; Li L. H.; Fiore A.; et al. Engineering of light confinement in strongly scattering disordered media. *Nat. Mater.* **2014**, 13, 720-725.

(15) Gao J.; Combrie S.; Liang B.; Schmitteckert P.; Lehoucq G.; Xavier S.; Xu X.; Busch K.; Huffaker D. L.; De Rossi A.; et al. Strongly coupled slow-light polaritons in one-dimensional disordered localized states. *Sci. Rep.* **2013**, 3, 1994.

(16) Vynck K.; Burresi M.; Riboli F.; Wiersma D. S. Photon management in two-dimensional disordered media. *Nat. Mater.* **2012**, 11, 1017-1022.

(17) Bertolotti J.; van Putten E. G.; Blum C.; Lagendijk A.; Vos W. L.; Mosk A. P. Non-invasive imaging through opaque scattering layers. *Nature* **2012**, 491, 232-234.

(18) Hughes S.; Ramunno L.; Young J.F.; Sipe J.E. Extrinsic optical scattering loss in photonic crystal waveguides: role of fabrication disorder and photon group velocity. *Phys. Rev. Lett.* **2005**, 94, 033903.

(19) Kuramochi E.; Notomi M.; Hughes S.; Shinya A.; Wanatabe T.; Ramunno L. Disorder-induced scattering loss of line-defect waveguides in photonic crystal slabs. *Phys. Rev. B* **2005**, 72, 161318(R).

(20) Patterson M.; Hughes S.; Combrie S.; Tran N.-V.-Q.; De Rossi A.; Gabet R.; Jaouen Y. Disorder-induced coherent scattering in slow-light photonic crystal waveguides. *Phys. Rev. Lett.* **2009**, 102, 253903.

(21) Moss D. J.; Morandotti R.; Gaeta A. L.; Lipson M. New CMOS-compatible platforms based on silicon nitride and Hydex for nonlinear optics. *Nat. Photonics* **2013**, 7, 597-607.

(22) Davanço M.; Ates S.; Liu Y.; Srinivasan K. Si_3N_4 optomechanical crystals in the resolved-sideband regime. *Appl. Phys. Lett.* **2014**, 104, 041101.

(23) Kistner J.; Chen X.; Weng Y.; Strunk H. P.; Schubert M. B.; Werner J. H. Photoluminescence from silicon nitride - no quantum effect. *J. Appl. Phys.* **2011**, 110, 023520.

(24) Barth M.; Nüsse N.; Stingl J.; Löchel B.; Benson O. Emission properties of high Q silicon nitride photonic crystal heterostructure cavities. *Appl. Phys. Lett.* **2008**, 93, 021112.

(25) Khan M.; Babinec T.; McCutcheon M.W.; Deotare P.; Lončcar M. Fabrication and characterization of high-quality-factor silicon nitride nanobeam cavities. *Optics Letters* **2011**, 36, 421-423.

(26) Sapienza L.; Davanço M.; Badolato A.; Srinivasan K. Nanoscale optical positioning of single quantum dots for bright and pure single-photon emission. *Nat. Commun.* **2015**, 6, 7833.

(27) Vasco J.P; Hughes S. Statistics of Anderson-localized modes in disordered photonic crystal slab waveguides. *Phys. Rev. B* **2017**, 95, 224202.

(28) Savona V. Electromagnetic modes of a disordered photonic crystal. *Phys. Rev. B* **2011**, 83, 085301.

(29) Chabanov A.A.; Stoychev M.,; Genack A.Z. Statistical signatures of photon localization. *Nature* **2000**, 404, 850-853.

(30) Makarova M.; Vučković J.; Sanda H.; Nishi Y. Silicon-based photonic crystal nanocavity light emitters. *Appl. Phys. Lett.* **2006**, 89, 221101.

(31) Murshidy M. M.; Adawi A. M.; Fry P. W.; Whittaker D. M.; Lidzey D. G. The optical properties of hybrid organic-inorganic L3 nanocavities. *J. Opt. Soc. Am. B* **2010**, 27, 215-221.

(32) Barth M.; Kouba J.; Stingl J.; Löchel B.; Benson O. Modification of visible spontaneous emission with silicon nitride photonic crystal nanocavities. *Opt. Express* **2007**, 15, 17231-17240.

(33) Sekoguchi H.; Takahashi Y.; Asano T.; Noda S. Photonic crystal nanocavity with a Q-factor of ∼9 million. *Opt. Express* **2014**, 22, 916-924.

(34) Hennessy K.; Badolato A.; Winger M.; Gerace D.; Atatüre M.; Gulde S.; Fält S. Hu

E. L.; Imamoğlu A. Quantum nature of a strongly coupled single quantum dot-cavity system. *Nature* **2007**, 445, 896-899.

(35) Pelton M. Modified spontaneous emission in nanophotonic structures. *Nat. Photonics* **2015**, 9, 427-435.

(36) Wiersma D.S. The physics and applications of random lasers. *Nat. Phys.* **2008**, 4, 359-367.

(37) Aichele T.; Zwiller V.; Benson O. Visible single-photon generation from semiconductor quantum dots. *New J. Phys.* **2004**, 6, 90.

(38) Xia F.; Wang H.; Xiao D.; Dubey M.; Ramasubramaniam A. Two-dimensional material nanophotonics. *Nat. Photonics* **2014**, 8, 899-907.

(39) Aharonovich I.; Greentree A.D.; Prawer S. Diamond Photonics. *Nat. Photonics* **2011**, 5, 397-405.

(40) Knowles H. S.; Kara D. M.; Atatüre M. Observing bulk diamond spin coherence in high-purity nanodiamonds. *Nat. Mater.* **2014**, 13, 21-25.

(41) Barclay P. E.; Fu, K.-M. C.; Santori C.; Faraon A.; Beausoleil R. G. Hybrid nanocavities for resonant enhancement of color center emission in diamond. *Phys. Rev. X* **2011**, 1, 011007.

(42) Knill E.; Laflamme R.; Milburn G.J. A scheme for efficient quantum computation with linear optics. *Nature* **2001**, 409, 46-52.

(43) Bertolotti J.; Gottardo S.; Wiersma D. S.; Ghulinyan M.; Pavesi L. Optical necklace states in Anderson localized 1D systems. *Phys. Rev. Lett.* **2005**, 94, 113903.

(44) Xu T.; Wu S. P.; Miloradovic I.; Therien M. J.; Blasie J. K. Incorporation of designed extended chromophores into amphiphilic 4-helix bundle peptides for nonlinear optical biomolecular materials. *Nano Lett.* **2006**, 6, 2387-2394.

(45) Carey A.-M.; Hacking K.; Picken N.; Honkanen S.; Kelly S.; Niedzwiedzki D. M.; Blankenship R. E.; Shimizu Y.; Wang-Otomo Z.-Y.; Cogdell R. J. Characterisation of the LH2 spectral variants produced by the photosynthetic purple sulphur bacterium Allochromatium vinosum. *Biochim. Biophys. Acta, Bioenerg.* **2014**, 1837, 1849-1860.

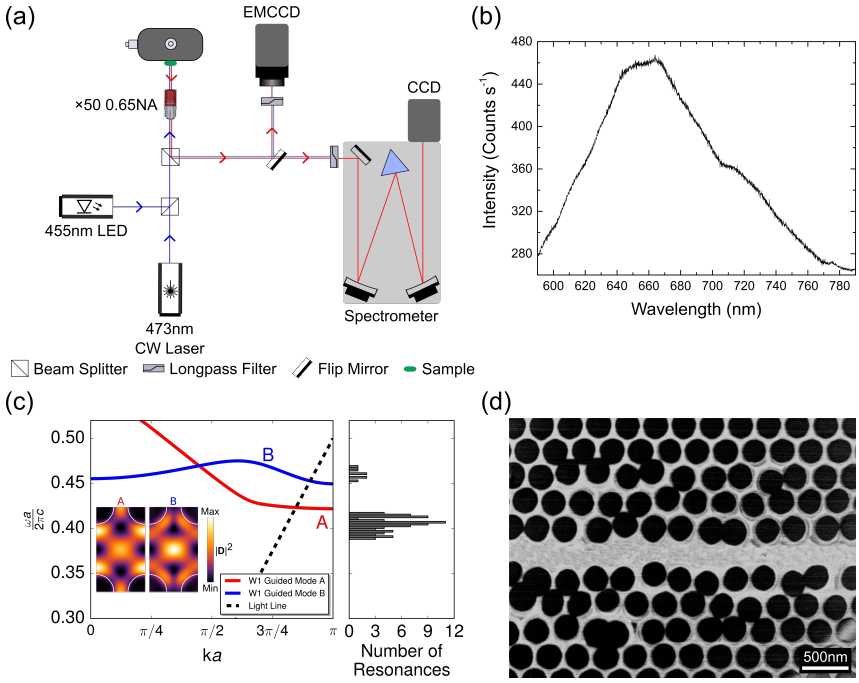

Figure 1: (a) Schematic of the confocal micro-photoluminescence set-up (not to scale), comprising a light emitting diode (LED) emitting around 455 nm and a continuous wave (CW) laser emitting at 473 nm as excitation sources, focused by a 50x microscope objective (with numerical aperture NA = 0.65) onto a sample placed on an xy-translation stage. The detection is carried out by an Electron Multiplying Charge Coupled Device (EMCCD) for photo-luminescence imaging and by a CCD at the exit port of a reflection grating spectrometer for spectral characterisation. (b) Photo-luminescence spectrum collected from an unpatterned area of the silicon nitride wafer, at room temperature, under laser excitation with a power density of 28 kW/cm^2. (c) Photonic band diagram calculations showing the guided modes of the perfectly periodic photonic crystal waveguide. Insets: Mode field intensity profiles ($\mathbf{D} = \varepsilon\mathbf{E}$, where $\mathbf{E}$ is the electric field and ε is the permittivity) calculated for the two guided modes at the edge of the Brillouin zone. The right panel shows the number of resonances experimentally measured in the waveguides with 0% disorder as a function of their scaled frequency. (d) Scanning Electron Microscope image of a fabricated photonic crystal waveguide where (10%) disorder is introduced by displacing, with respect to the perfectly periodic structure, the position of the holes in the three rows above and below the row of missing holes.

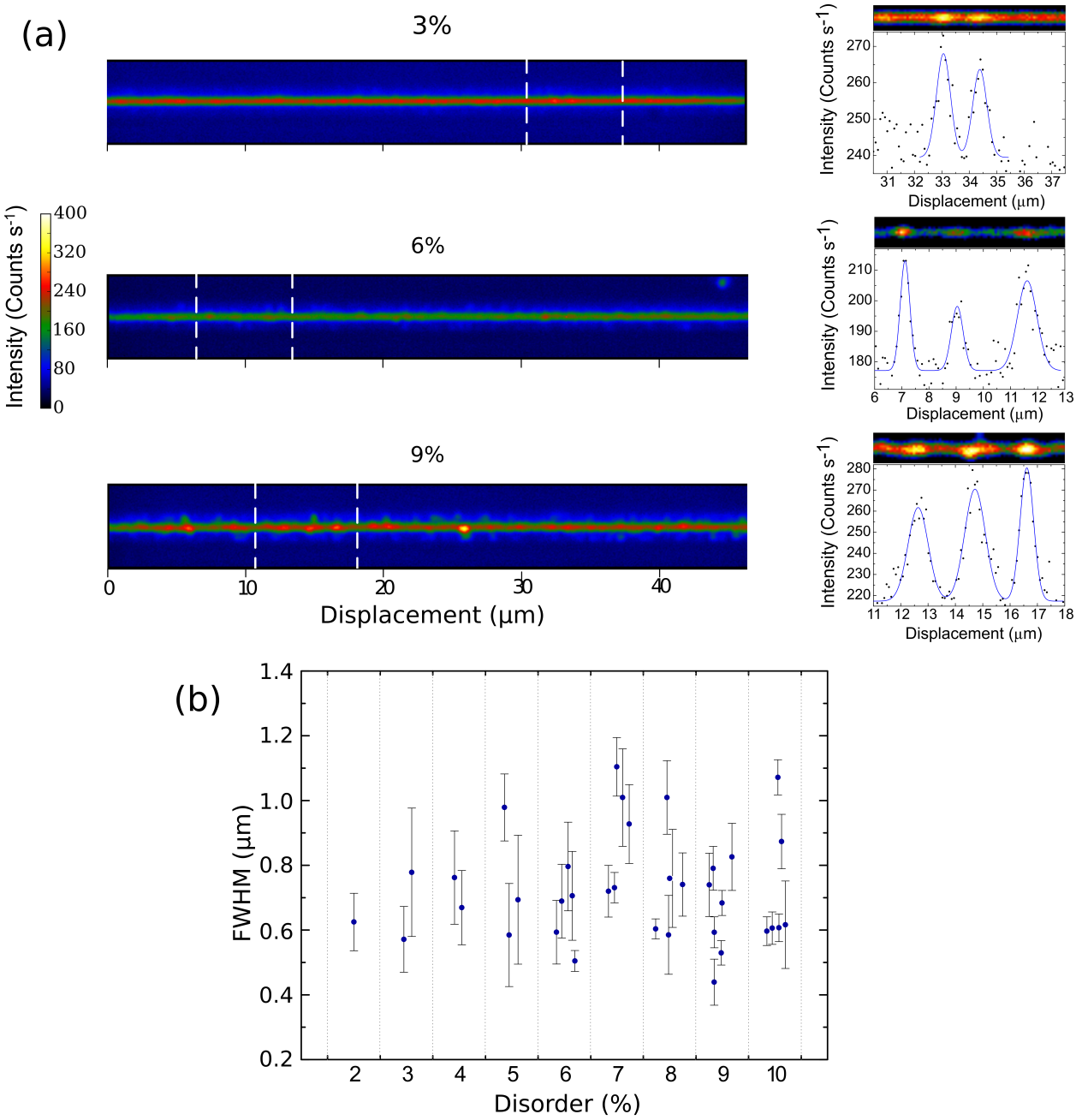

Figure 2: (a) Left panels: Photo-luminescence images of the emission from waveguides with different degrees of disorder (3%, 6%, 9%), collected at room temperature, under light emitting diode illumination with a power density of 40 W/cm^2. Right panels: Enlargement of the areas highlighted by the dashed lines in the left panels and horizontal linecuts along the centre of the waveguides (circles) and their Gaussian fits (solid lines). (b) Statistics of the spatial extension (Full Width at Half Maximum, FWHM, of the Gaussian fits) of the peaks observed in the photo-luminescence images, plotted as a function of the degree of disorder (horizontally offset for clarity). The error bars represent the standard deviation of the FWHM extracted from the fits.

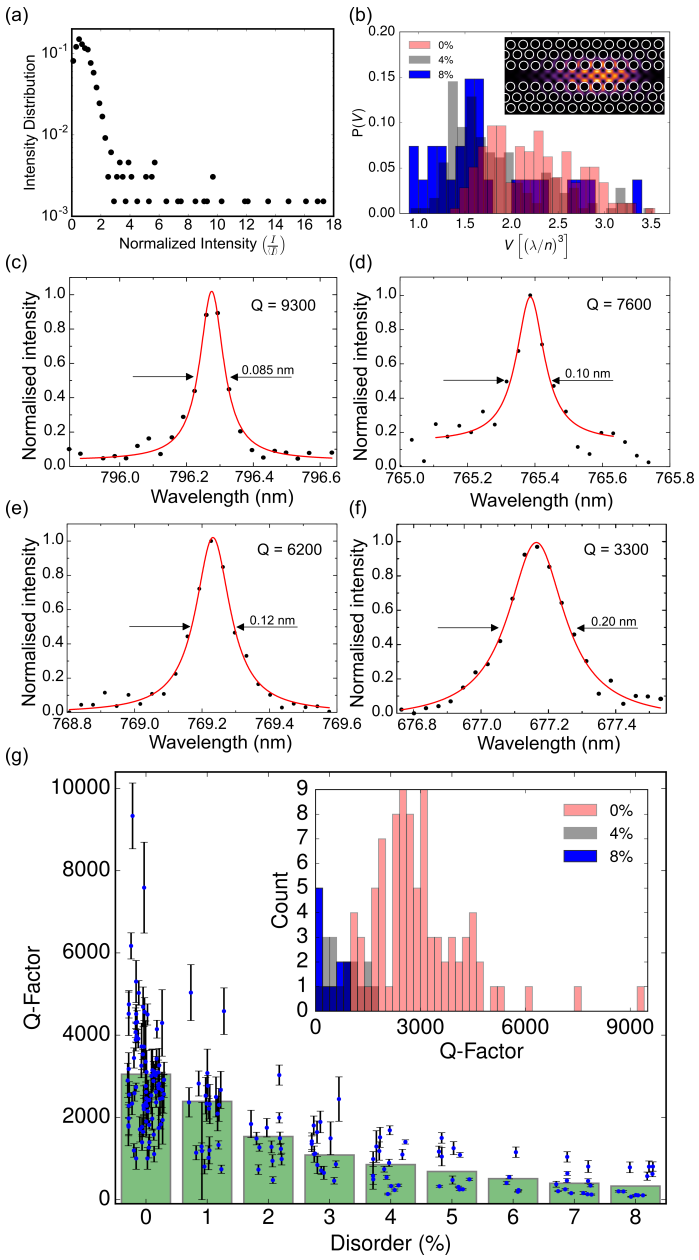

Figure 3: (a) Probability distribution of the normalised photo-luminescence intensity measured on a sample with 0% disorder. (b) Calculated probability distributions P of the mode volumes V of the Anderson-localised modes for 0, 4, 8 % disorder. Inset: Image of the mode profile calculated for the perfectly periodic photonic crystal structure. (c-f) Examples of the normalised spectral resonances (symbols) and their Lorentzian fits (solid lines). The arrows indicate the full width at half maxima of the peaks. (g) Statistics of the quality factors as a function of degree of disorder (horizontally offset for clarity). The values are extracted from Lorentzian fits, like the ones shown in panel (b), and the error bars represent the standard deviation obtained by propagating the uncertainty in the linewidth and in the central wavelength obtained from the fits. The histograms show the mean value of the calculated quality factors for the different degrees of disorder. The inset shows histograms of the number of events (count) as a function of quality factor, for different degrees of disorder (0%, 4% and 8%).